Published in final edited form as:
Clin Exp Metastasis. 2014 February ; 31(2): 247–256. doi:10.1007/s10585-013-9625-2.

Prostate cancer derived prostatic acid phosphatase promotes an osteoblastic response in the bone microenvironment

Sandy R. Larson,
Genitourinary Cancer Research Laboratory, Department of Urology, University of Washington, Box 356510, Seattle, WA 98195, USA

Jessica Chin,
Genitourinary Cancer Research Laboratory, Department of Urology, University of Washington, Box 356510, Seattle, WA 98195, USA

Xiaotun Zhang,
Genitourinary Cancer Research Laboratory, Department of Urology, University of Washington, Box 356510, Seattle, WA 98195, USA

Lisha G. Brown,
Genitourinary Cancer Research Laboratory, Department of Urology, University of Washington, Box 356510, Seattle, WA 98195, USA

Ilsa M. Coleman,
Fred Hutchinson Cancer Research Center, Seattle, WA, USA

Bryce Lakely,
Genitourinary Cancer Research Laboratory, Department of Urology, University of Washington, Box 356510, Seattle, WA 98195, USA

Martin Tenniswood,
University of Albany, Albany, NY, USA

Eva Corey,
Genitourinary Cancer Research Laboratory, Department of Urology, University of Washington, Box 356510, Seattle, WA 98195, USA

Peter S. Nelson,
Fred Hutchinson Cancer Research Center, Seattle, WA, USA

Department of Medicine, University of Washington, Seattle, WA, USA

Robert L. Vessella, and
Genitourinary Cancer Research Laboratory, Department of Urology, University of Washington, Box 356510, Seattle, WA 98195, USA

Department of Veterans Affairs Medical Center, Seattle, WA, USA

Colm Morrissey
Genitourinary Cancer Research Laboratory, Department of Urology, University of Washington, Box 356510, Seattle, WA 98195, USA

Correspondence to: Colm Morrissey, cmorriss@u.washington.edu.

Electronic supplementary material The online version of this article (doi:10.1007/s10585-013-9625-2) contains supplementary material, which is available to authorized users.

Conflict of interest The authors declare that they have no conflict of interest.

Colm Morrissey: cmorriss@u.washington.edu

Abstract

Approximately 90 % of patients who die of prostate cancer (PCa) have bone metastases, often promoting osteoblastic lesions. We observed that 88 % of castration-resistant PCa (CRPC) bone metastases express prostatic acid phosphatase (PAP), a soluble secreted protein expressed by prostate epithelial cells in predominately osteoblastic (n = 18) or osteolytic (n = 15) lesions. Additionally, conditioned media (CM) of an osteoblastic PCa xenograft LuCaP 23.1 contained significant levels of PAP and promoted mineralization in mouse and human calvaria-derived cells (MC3T3-E1 and HCO). To demonstrate that PAP promotes mineralization, we stimulated MC3T3-E1 cells with PAP and observed increased mineralization, which could be blocked with the specific PAP inhibitor, phosphonic acid. Furthermore, the mineralization promoted by LuCaP 23.1 CM was also blocked by phosphonic acid, suggesting PAP is responsible for the mineralization promoting activity of LuCaP 23.1. In addition, gene expression arrays comparing osteoblastic to osteolytic CRPC (n = 14) identified betacellulin (BTC) as a gene upregulated during the osteoblastic response in osteoblasts during new bone formation. Moreover, BTC levels were increased in bone marrow stromal cells in response to LuCaP 23.1 CM in vitro. Because new bone formation does occur in osteoblastic and can occur in osteolytic CRPC bone metastases, we confirmed by immunohistochemistry (n = 36) that BTC was highly expressed in osteoblasts involved in new bone formation occurring in both osteoblastic and osteolytic sites. These studies suggest a role for PAP in promoting the osteoblastic reaction in CRPC bone metastases and identify BTC as a novel downstream protein expressed in osteoblasts during new bone formation.

Keywords

Bone; Betacellulin; Metastases; Osteoblastic; PAP; Prostate cancer

Introduction

Prostate Cancer (PCa) preferentially metastasizes to the bone, with bone involvement occurring in 90 % of patients with metastatic disease. These metastases cause severe bone pain, replacement of bone marrow, pathologic fracture and spinal cord compression [1, 2]. The evaluation of bone metastases obtained through studies of rapid autopsies have confirmed that in these metastatic sites bone turnover is increased; however, the new bone forms layers of fragile, woven bone with reduced mechanical strength [3–5]. In concert with the heterogeneity of bone formation, there is a wide spectrum of responses to treatment. A number of therapies have been developed to address osteolytic bone metastases, such as bisphosphonates (e.g. zoledronic acid), and more recently RANKL inhibitors (e.g. Denosumab) [6–9]. Additionally, a number of factors have been described as possible targets to treat osteoblastic bone metastases including, but not limited to ET-1, Wnt signaling proteins and the TGF-β superfamily, including the BMPs [8–12]. While these proteins promote bone formation in vitro, the specific mechanisms that promote bone growth in PCa patients are largely unknown. Therefore, much focus has been on targeting soluble proteins secreted from tumor cells that promote bone growth within the bone-tumor microenvironment.

One of the major proteins secreted by normal prostatic epithelium and PCa tumor cells is prostatic acid phosphatase (PAP). In 1936, Gutman et al. described an increase of phosphatase activity at osteoblastic skeletal metastatic sites, indicating that the production of phosphatases may play an important role in dictating the osteoblastic behavior of bone metastasis. It was subsequently described that when added to cell culture, PAP stimulated collagen synthesis and alkaline phosphatase production in osteoprogenitor cells and

osteoblasts, leading to the hypothesis that PAP may directly stimulate bone forming cells, likely contributing to the sclerotic pattern at sites of PCa bone metastases [13]. More recently, it was shown that secreted PAP was expressed in clinical osteosclerotic PCa bone metastases themselves, and therefore proposed that PAP may play a causal role in the osteoblastic nature of PCa bone metastases [14].

We have shown previously that the relative expression of numerous—rather than a single-bone remodeling proteins may determine the bone response in PCa skeletal metastases [11]. In the current study, we confirm the expression of PAP in clinical castration-resistant PCa (CRPC) bone metastases and PCa xenograft models. Furthermore, using the osteoblastic LuCaP 23.1 PCa xenograft, we generated data supporting the hypothesis that PAP secreted by tumor cells has the potential to promote the osteoblastic response in PCa metastases. We also identify genes promoting bone formation (including betacellulin (BTC)) altered in osteoblasts in response to PCa xenograft LuCaP 23.1 conditioned medium (CM). Lastly, we describe the expression of BTC and BTC-associated proteins during new bone formation in CRPC metastases [15–17].

Materials and methods

Preparation and characterization of LuCaP PCa xenografts

MEM was conditioned for 48 h with 0.05 g/ml minced Lu-CaP tumor tissue from eight different LuCaP PCa xenograft lines (LuCaP 23.1, 35, 58, 70, 86.2, 136, 141 and 145.1), supplemented with 10 %FBS, 10 mM β-glycerol phosphate in HBSS, and 50 μg/ml L-ascorbic acid. Conditioned media (CM) was centrifuged for 10 min at 16,000 RCF, filtered through a 2 μm filter and used for mass spectrometry. In addition, to determine which CM promoted mineralization in vitro, 2 ml of CM was added to wells containing MC3T3-E1 cells (osteoblastic precursor cell line derived from mouse calvaria), seeded in a six-well plate at 100,000 cells per well, and allowed to come to confluence. Control wells of each plate were treated with mineralization media (MM) (10 %FBS in MEM with 10 mM β-glycerol phosphate in HBSS [Sigma Chemical Co., St. Louis, MO], and 50 μg/ml L-ascorbic acid). Mineralization was determined by Alizarin Red assay as described below.

Mass spectrometry

Conditioned media was used for mass spectrometry. The proteins from the CM were precipitated, alkylated, and after tryptic digestion the peptide mixture was desalted using Sepak C18 cartridge. The eluent was fractionated by SCX column to ten fractions. The fractions were concentrated, and reconstituted in 10 μl of 5 % formic acid for LC–MS/MS analysis.

HPLC: CapLC (Waters, USA) Column: Vydac C18 (5 μm, 100 mm ID × 150 mm, Vydac, CA) Trapping column: Vydac C18 EV 300 A, 10 um Solvent A: 5 % CH_3CN + 0.1 % formic acid + 0.01 % TFA Solvent B: 85 % CH_3CN + 10 % isopropanol + 5 % H_2O + 0.1 % formic acid + 0.01 % TFA Flow rate: 250 nl/min Gradient: 100 min linear gradient from 10 to 100 % B MS/MS: Q-TOF2 (Micromass/Waters, USA). Peak list was created using Mascot Distiller 2.3 software from Matrix Science with a processing macro that smoothes, centroids, and assesses the quality of data. In house MASCOT 2.3 from Matrix Science (London, UK) was used to assist the interpretation of tandem mass spectra against the IPI mouse database. Variable modifications including deamidation (N, Q), oxidation (M), and carbamidomethylation (C) were considered for the searching.

Alizarin red mineralization assays

Cultured cells—HCO (human calvaria cells) or MC3T3-E1—were seeded at 50,000 cells/well in MEM and 10 %FBS. Mineralization media (MM) was added to all cultures 1–2 days after seeding and replaced every other day. MM, LuCaP 23.1 CM (5, 10 or 20 %), Prostatic acid phosphatase, lyophilized powder obtained from human prostatic fluid (CSI14633A; Cell Sciences, Canton, MA) or phosphonic acid, P-[phenyl[(phenyl methyl)amino]methyl]—(CAS#25881-35-0; Aurora Fine Chemicals LLC, SanDiego, CA) was added to cultures typically on day 5–6, before mineralization occurred. After mineralization, cells were fixed in 10 % formalin for 20 min and then washed. 2 % alizarin red was added to air-dried plates. After washing, retained dye was extracted in a solution of 20 % methanol and 10 % acetic acid in water, and absorbance measured at 405 nm was measured.

Tissue acquisition and processing

Human PCa metastasis were obtained as part of the University of Washington Medical Center PCa Donor Rapid Autopsy Program, which is approved by the University of Washington Institutional Review Board [18]. To assess PAP expression in PCa metastases, we stained a tissue microarray consisting of 160 metastatic sites from 50 patients (83 bone metastases and 77 soft tissue metastases). To compare PAP expression in highly osteoblastic and osteolytic PCa bone metastases, thirty-three bone samples from rapid autopsies of 30 patients who died with a diagnosis of metastatic CRPC were processed. From 30 patients (n = 33), metastatic cores were isolated at autopsy and divided into two portions—one flash frozen in liquid nitrogen to be used for RNA isolation and one decalcified in formic acid, fixed in 10 % neutral buffered formalin and embedded in paraffin used for immunohistochemistry (IHC). From a selected subset of 11 patients, seven bone metastases were identified as highly osteoblastic and seven as highly osteolytic. The corresponding frozen tissue was used for RNA isolation. Macroscopic assessment of paraffin embedded tissues from the same bone cores confirmed specimens to be at least 90 % tumor. Clinical data associated with these samples can be found in our recent publication [11]. LuCaP xenograft tumored tibae were processed in similar fashion to the patient metastatic bone cores.

RNA amplification and microarray hybridization

To determine the effect of LuCaP 23.1 CM on mineralization, human bone marrow stromal cells (BMSC) isolated from normal bone marrow aspirates of three patients were seeded at 100,000 cells/well, allowed to come to confluence and then treated with mineralization medium (Medium was replaced every third day). Cultures were then treated with LuCaP 23.1 CM for 48 h or with MM alone. Total RNA was extracted using STAT-60 (Tel-Test, INC. Friendswood, TX) according to the manufacturer's protocol. A reference standard RNA for use in two-color oligo arrays was prepared and total RNA from BMSC as well as reference total RNA samples were amplified and hybridized to Agilent 44K whole human genome expression oligonucleotide microarray slides as previously described [11]. The Statistical Analysis of Microarray (SAM) program was used to analyze expression differences between CM and MM groups using unpaired, two-sample t-tests on all probes passing filters and controlled for multiple testing by estimation of q-values using the false discovery rate (FDR) method [19]. Microarray data are deposited in the Gene Expression Omnibus database under the accession number GSE48907. To compare to profiles of human osteoblastic and osteolytic bone metastases, an expression dataset containing 14 bone metastases previously published under the GEO accession GSE41619 was used [11].

Quantitative reverse transcription-polymerase chain reaction (qRT-PCR)

Primers (Integrated DNA Technologies, Coralville, IA) (Online Resource 1) were designed to span intron–exon boundaries using Primer3 software (http://frodo.wi.mit.edu). One microgram of either amplified or total RNA from each sample was reverse transcribed into cDNA using the Advantage RT-for-PCR kit for random hexamer priming according to manufacturer's protocol (BD Biosciences, Palo Alto, CA). Reactions contained 10 μl of Absolute QPCR SYBR Green Mix (Thermo Scientific, Wilmington, DE), 2 μl of cDNA template (1:10 dilution of reverse transcribed RNA), 0.4 μl each of forward and reverse primer (200 nM) and 7.2 μl H_2O. qRT-PCR was performed on a Rotor-Gene RG-3000 (Corbett Research, Sydney, Australia) using the following parameters: 95 °C for 15 min followed by 40 cycles of denaturing at 95 °C for 15 s and annealing/extension at T(m)/72 °C for 30 s each. qRT-PCR quality was accessed using a four-fold dilution standard curve of LuCaP 23.1 cDNA with a R^2 value >0.99. Amplicon product was confirmed by melt curve analysis and gel electrophoresis. Using cycle threshold values, average expression levels were normalized against β-actin. Fold changes and significance using paired t-tests were determined between experimental groups.

Immunohistochemistry

Formalin-fixed paraffin-embedded tissue sections (5 μm) were deparaffinized and rehydrated. Antigen retrieval was performed with 10 mM citrate buffer (pH 6.0) in a pressure cooker (20 psi for 5 min) as needed. Endogenous peroxide was quenched by 3 % H_2O_2 for 15 min and avidin/biotin were blocked respectively with corresponding reagents (Vector Laboratories Inc.). After incubation with 5 % normal goat-horse-chicken serum at room temperature for 1 h, primary antibodies, PAP (Abcam, Ab75704) or BTC (R&D Systems, Inc., ANU02) were added at 4 °C overnight followed by biotinylated secondary antibody (1:150) (Vector Laboratories Inc.) and ABC reagent (Vector Laboratories Inc.), 30 min each. DAB (Invitrogen Corp.) was used as chromogen. All sections were counterstained with hematoxylin and mounted with Cytoseal XYL (Richard Allan Scientific). Mouse or goat IgG was used at the same concentration as the primary antibody for negative controls.

Immunohistochemical assessment and analysis

Immunostaining was assessed using a quasi continuous score system, created by multiplying each intensity level ("0" for no brown color, "1" for faint and fine brown chromogen deposition, and "2" for clear and coarse granular chromogen clumps) with the corresponding percentage of cells expressing the particular intensity, and then summing all values to final score for each sample (scores ranging from 0 to 200) [19]. The distribution of the final scores were grouped as "none" (score range: 0), "weak" (score range: 0–100), "moderate" (score range: 100–150) and "intense" (score range: 150–200). Missing or damaged sections were excluded from analysis. Significance of differences were calculated using a paired t-test, with p values ≤0.05 indicating statistical significance.

Results

LuCaP 23.1 prostate carcinoma conditioned media induces mineralization and contains PAP

The PCa xenograft lines, LuCaP 23.1, LuCaP 58, and LuCaP 136 elicit osteoblastic reactions in murine tibiae: LuCaP 35 displays a mixed bone response and LuCaP 70, LuCaP 86.2, LuCaP 141 and LuCaP 145.1 are osteolytic (data not shown). When evaluating PAP expression in LuCaP models in the bone environment (intra-tibial), Lu-CaP 23.1, LuCaP 70, LuCaP 86.2 and LuCaP 141 displayed intense PAP staining; LuCaP 58 and LuCaP 136 exhibited moderate staining. Only LuCaP 35 and LuCaP 145.1 intra-tibial tumors had weak

to no expression (Online Resource 2). Because the microenvironment can influence gene expression, we also stained subcutaneous LuCaP tumors for PAP (Online Resource 2). LuCaP 23.1 exhibited strong immunoreactivity, however the two other osteoblastic xenograft lines (LuCaP 58 and LuCaP 136) did not exhibit any subcutaneous PAP immunoreactivity. LuCaP 86.2 and LuCaP 141 also exhibited strong immunoreactivity for PAP, LuCaP 35 displayed moderate PAP immunoreactivity, while LuCaP 70 and the neuroendocrine LuCaP 145.1 displayed either weak or no PAP expression in subcutaneous tumors. The disparity of PAP expression specifically for LuCaP 58 and LuCaP 136 between the intra-tibial and subcutaneous LuCaP tumors shows importance of the bone microenvironment's influence on tumor phenotypes including protein expression. Conditioned media (CM) isolated from subcutaneous tumor cells cultured in vitro for each of these xenograft lines was added to mouse MC3T3-E1 cells and of the eight lines, only LuCaP 23.1 induced mineralization (Fig. 1a). As stated previously no PAP expression was observed in the osteoblastic LuCaP 58 and LuCaP 136 subcutaneous tumors. Mass spectrometry of the CM from each of the eight LuCaP subcutaneous tumors verified this by revealing that PAP was detected only in LuCaP 23.1 CM (data not shown). Additionally, we determined that LuCaP 23.1 CM also induced mineralization by human osteoblasts (HCO) in culture ($p = 0.0079$) (Fig. 1b, c).

LuCaP 23.1 conditioned media promotes osteoblastic gene expression

To evaluate the influence of PCa cells on bone marrow stromal cells (BMSC) we exposed BMSC to mineralization media (MM) or LuCaP 23.1 CM, extracted RNA and quantitated transcript levels by microarray hybridization. Exposure to LuCaP 23.1 CM increased the expression of 174 genes decreased the expression of 644 genes (q-value of 10 %). Fourteen genes previously shown to be expressed in osteoblasts or involved in bone remodeling were selected for validation by qRT-PCR (Fig. 2a) [12, 20–31]. By qRT-PCR when normalized to MM alone, TGM2, EPHA4, SDC1, CCL20, BMP2, STC1, PDPN, SPP1, ENPP1 and VEGFA were significantly upregulated in presence of LuCaP 23.1 CM ($p < 0.05$), consistant with the gene expression array analysis (Fig. 2b). Conversely, ASPN, PTN, ROR1, and OSR2 were significantly downregulated in the presence of LuCaP 23.1 CM ($p < 0.05$), also consistant with the microarray analysis.

PAP induces mineralization in vitro

We detected high PAP levels in LuCaP 23.1 CM, therefore our next focus was to determine if PAP contributes to mineralization induced by the LuCaP 23.1 CM. Mouse osteoblast-like MC3T3-E1 cells were treated with 0.05, 0.025 and 0.0125 units of PAP (Fig. 3). Compared to control, 0.05 units of PAP treatment induced a significant 3.7 fold increase in mineralization ($p = 0.005$) when compared to control.

Phosphonic acid blocks LuCaP 23.1-induced mineralization in vitro

The benzylaminophosphonic acids are inhibitors of PAP [32]. Vovk et al. have demonstrated that the R enantiomer of P-[phenyl[(phenyl methyl)amino]methyl]- is a potent inhibitor of PAP [33]. To determine if the PAP inhibitor P-[phenyl[(phenyl methyl)amino]methyl]-(phosphonic acid; PA) had an indirect effect on MC3T3-E1 mineralization, phosphonic acid was added to MC3T3-E1 cells at concentrations ranging from 25 μM down to 0.2 μM. No significant inhibition of mineralization occurred at 25 μM down to 0.2 μM (Fig. 4a). Next, PA was added to MC3T3-E1 cells treated with 0.05 units of PAP at concentrations of PA ranging from 25 to 0.2 μM, to confirm its inhibitory potential. There was a dramatic reduction in mineralization in the 25, 12.5, 6.25 and 3.15 μM concentrations of PA (decreasing mineralization by 97.6, 95.6, 92.1 and 97.9 % respectively), with PA having a significant effect on mineralization down to 0.4 μM (Fig.

4b). We had previously determined that 1 % LuCaP 23.1 CM was not sufficient to induce mineralization in MC3T3-E1 cells and that 5 % LuCaP 23.1 CM would promote mineralization in MC3T3-E1 cells (data not shown). To determine if PA would reduce LuCaP 23.1 CM associated mineralization we treated MC3T3-E1 cells with 5–20 % LuCaP 23.1 CM with 5 μM PA. PA significantly reduced mineralization in MC3T3-E1 cells treated with 5, 10 or 20 % LuCaP 23.1 CM, suggesting PAP is the active protein driving mineralization in LuCaP 23.1 CM (Fig. 4c).

PAP expression is not limited to osteoblastic PCa bone metastases

PAP protein expression was analyzed by IHC from 30 patients in highly osteoblastic (n = 18) or highly osteolytic (n = 15) samples (Fig. 5a), and shown to be expressed in 88 % of the CRPC bone metastases. There was no significant difference between PAP expression in the osteoblastic versus osteolytic samples (Fig. 5b). However, expression of PAP was higher in bone metastases compared to other metastatic sites, such as liver ($p < 0.001$) and lymph nodes ($p < 0.001$) with no difference observed between bone and other sites (appendix, kidney and lung) (Fig. 5c). Furthermore, gene expression analysis and qRT-PCR results revealed that transcript levels of ACPP in seven highly osteoblastic and seven highly osteolytic clinical specimens, although present, displayed no significant differential expression between osteoblastic and osteolytic tissues (Fig. 6).

Betacellulin is associated with new bone formation in PCa bone metastases

Gene expression array results and qRT-PCR from the patient samples (Fig. 6) identified a novel bone formation-associated secreted factor—betacellulin (BTC)—that could be responsible, at least in part, for the osteoblastic response in in vivo CRPC bone metastasis (Fig. 6). Additionally, BTC was significantly upregulated over eightfold in response to LuCaP 23.1 CM in vitro cultures (Fig. 2b). Therefore, we also examined the expression of BTC-associated genes in the same samples. On the gene expression arrays, vascular endothelial growth factor A (VEGFA), and BTC were among the top secreted factors that were highly expressed in the osteoblastic versus osteolytic clinical metastases. Three other related factors, epidermal growth factor receptor (EGFR), vascular endothelial growth factor B (VEGFB) and hypoxia inducible factor alpha (HIF1A) were not differentially expressed on the gene expression arrays. Using qRT-PCR, we confirmed that VEGFA transcripts were upregulated in osteoblastic samples with a 2.77 fold increase however this only had a trend towards significance ($p = 0.067$). BTC was significantly upregulated with a 4.26 fold increase ($p = 0.041$) in osteoblastic metastases compared to osteolytic metastases. EGFR, VEGFB and HIF1A transcript levels did not display any significant difference between osteoblastic and osteolytic samples by qRT-PCR (fold changes 2.19, 1.22 and 1.47, $p = 0.131$, $p = 0.659$ and 0.377, respectively). Upon further analysis of clinical CRPC bone metastases (n = 36) by immunohistochemistry, we identified 15 metastatic sites with newly formed woven bone in both osteoblastic and osteolytic samples. These new bones had eosinophilic staining in H&E sections, and consisted of a higher percentage of osteocytes than normal bone. By IHC, BTC expression was congruent with new bone formation, and was associated with osteoblasts, osteocytes and was present at the new bone surface. Active stromal cells adjacent to the new bone also had similar intense BTC staining. In contrast, the lamellar bone, from where the new bone was derived was negative for BTC. (Fig. 7, Online Resource 3).

Discussion

We have demonstrated that the highly osteoblastic PCa xenograft line, LuCaP 23.1, secretes PAP at significant levels and promotes mineralization in vitro. Furthermore, the PAP specific inhibitor phosphonic acid blocked the mineralization of MC3T3-E1 cells caused by

LuCaP 23.1 CM. This demonstrates that PAP is the soluble protein secreted by the highly osteoblastic LuCaP 23.1 PCa tumor cells that promotes mineralization in vitro. In addition we have demonstrated that the majority of CRPC metastases express PAP, that PAP is expressed in osteolytic and osteoblastic CRPC metastases, and that PAP is expressed at higher levels in the bone versus soft tissue. Furthermore, using xenograft models, we also found increased expression of PAP in prostate tumors growing in the bone microenvironment compared to tumors in a subcutaneous location. This emphasizes important influences of the tumor environment and further supports the conclusion that PAP is involved in bone remodeling and is associated with PCa bone metastases.

PAP expression in both osteoblastic and osteolytic PCa bone metastases does not contradict our hypothesis that PAP is involved in the osteoblastic reaction associated with PCa. While PAP promotes mineralization, its activity could be suppressed by osteolytic factors. We have previously shown that the overall bone response in CRPC bone metastases is likely caused by a combination of bone formation and bone degrading proteins, rather than a single protein [11]. Therefore, while PAP is expressed in osteoblastic and osteolytic bone metastases, this prostate specific protein may still drive the predominantly osteoblastic response in CRPC (independently or in combination with other factors) while at times be suppressed (in mixed lesions) or negated (in osteolytic lesions) by other osteolytic factors present in the bone microenvironment (e.g. DKK-1, sFRP-1, and RANKL) [34–36].

Although PAP is thought to be involved in androgen-dependent PCa progression, recently TGF-β_1, has been shown to upregulate PAP mRNA, suggesting an androgen-independent regulation of PAP expression [37]. The TGF-β signaling pathway promotes the proliferation and initial differentiation of osteoblasts [38]. The TGF-β type II receptor can be modulated by the TGFβ receptor interacting protein-1 (TRIP-1), which has a high affinity for the secreted osteoclast enzyme, tartrate resistant acid phosphatase 5b (TRAP) controlling osteoblast activity when coupled during bone remodeling at sites of resorption [38, 39]. This suggests that PAP may be acting in a similar fashion as the coupling mechanism between TRIP-1 and TRAP, mediating TGF-β_1, recruiting and activating osteoblasts to promote bone formation. An alternative mechanism of PAP's activity could be through ErbB-2. Interestingly, PAP has been demonstrated to interact with and dephosphorylate pTyr1221/2 of ErbB-2 thereby blocking downstream signaling of ERK1/2, Akt, Src, STAT-3 and STAT-5 [37, 40]. ErbB-2 phosphorylation has been shown to be reduced in mineralizing osteoblasts [41].

In addition to identifying PAP as a driver of the osteoblastic response in CRPC, we discovered that BTC is directly associated with new bone formation in CRPC bone metastases, suggesting a novel role for BTC. BTC has previously been associated with increased bone mass in BTC transgenic mice [17]. BTC (an EGF family ligand) can interact with the homodimers ErbB-1 and ErbB-4, as well as activate the heterodimers ErbB-1/ErbB-2, ErbB-1/ErbB-3, ErbB-1/ErbB-4, ErbB-2/ErbB-3 and ErbB-2/ErbB-4 [16, 42]. While blocking EGFR/ErbB-1 has been shown to antagonize BTC activity in some systems, inhibiting EGFR/ErbB-1 signaling has a limited effect on promoting tumor regression in clinical PCa bone metastases [43]. Interestingly, a secreted form of ErbB-3 has been implicated to be involved in bone formation and osteoblast differentiation in PCa [44]. Additionally, BTC induces angiogenesis through the activation of ErbB-2, ErbB-3 and ErbB-4 receptors, acting on the phosphatidylinositol 3′kinase/Akt pathway [16]. VEGF is also known to enhance both angiogenesis and bone formation [45]. To determine if there was an association between BTC, bone formation, angiogenesis, and VEGF, we evaluated VEGF expression in osteoblastic versus osteolytic metastases. While VEGF was not significantly different there was a trend towards higher VEGF expression in the osteoblastic

metastases. These data suggest an association of BTC with both angiogenesis and bone formation may be central to the osteoblastic response in CRPC bone metastases.

In conclusion we have demonstrated that osteoblastic LuCaP 23.1 PCa xenograft cells promote the mineralization in osteoblasts in vitro and that these cells secrete high levels of PAP. Furthermore, we have also shown that the mineralization caused by LuCaP 23.1 can be blocked by the PAP specific inhibitor phosphonic acid. In addition, we have also shown that PCa bone metastases from patients and xenograft models of PCa grown in bone express high levels of PAP, and that PAP levels are higher in bone metastases versus soft tissue metastases, and in intra-tibial LuCaP tumors versus subcutaneous LuCaP tumors. Interestingly, our data also show that PAP is not significantly higher in osteoblastic clinical bone metastases when compared to osteolytic bone metastases, implying that while PAP appears to drive the osteoblastic response, it can be moderated or negated by osteolytic factors secreted within the tumor microenvironment. Furthermore, the novel linkage of BTC to new bone formation provides a possible mechanism by which PAP drives the osteoblastic response. Taken together, these findings provide an explanation for the predominantly osteoblastic, but in some cases mixed, and osteolytic bone response observed in PCa bone metastases that are not typically observed in other solid tumor types.

Supplementary Material

Refer to Web version on PubMed Central for supplementary material.

Acknowledgments

We would like to thank Drs. Celestia Higano, Paul Lange, Bruce Montgomery, Martine Roudier and Lawrence True for their contributions to the University of Washington Medical Center Prostate Cancer Donor Rapid Autopsy Program. Additionally, we thank Ruth Dumpit, Gregory Mize, Holly Nguyen and Jennifer Noteboom for excellent technical assistance with this study. This material is the result of work supported by resources from the VA Puget Sound Health Care System, Seattle, Washington. This research was supported by funding by the Pacific Northwest Prostate Cancer SPORE (P50CA97186), the PO1 NIH grant (PO1CA085859), and a generous donation from Jim and Catherine Allchin and the Richard M. LUCAS Foundation.

References

1. Bubendorf L, Schopfer A, Wagner U, et al. Metastatic patterns of prostate cancer: an autopsy study of 1,589 patients. Hum Pathol. 2000; 31:578–583. [PubMed: 10836297]
2. Nieder C, Haukland E, Pawinski A, Dalhaug A. Pathologic fracture and metastatic spinal cord compression in patients with prostate cancer and bone metastases. BMC Urol. 2010; 10:23. [PubMed: 21176198]
3. Roudier MP, Morrissey C, True LD, Higano CS, Vessella RL, Ott SM. Histopathological assessment of prostate cancer bone osteoblastic metastases. J Urol. 2008; 180:1154–1160. [PubMed: 18639279]
4. Jin JK, Dayyani F, Gallick GE. Steps in prostate cancer progression that lead to bone metastasis. Int J Cancer. 2011; 128:2545–2561. [PubMed: 21365645]
5. Morrissey C, Roudier MP, Dowell A, et al. Effects of androgen deprivation therapy and bisphosphonate treatment on bone in patients with metastatic castration-resistant prostate cancer: results from the University of Washington Rapid Autopsy Series. J Bone Miner Res. 2013; 28:333–340. [PubMed: 22936276]
6. Fizazi K, Carducci M, Smith M, et al. Denosumab versus zoledronic acid for treatment of bone metastases in men with castration-resistant prostate cancer: a randomised, double-blind study. Lancet. 2011; 377:813–822. [PubMed: 21353695]
7. Lee RJ, Saylor PJ, Smith MR. Treatment and prevention of bone complications from prostate cancer. Bone. 2011; 48:88–95. [PubMed: 20621630]

8. Valkenburg KC, Steensma MR, Williams BO, Zhong Z. Skeletal metastasis: treatments, mouse models, and the wnt signaling. Chin J Cancer. 2013; 32:380–396. [PubMed: 23327798]
9. Sturge J, Caley MP, Waxman J. Bone metastasis in prostate cancer: emerging therapeutic strategies. Nat Rev Clin Oncol. 2011; 8:357–368. [PubMed: 21556025]
10. Bagnato A, Loizidou M, Pflug BR, Curwen J, Growcott J. Role of the endothelin axis and its antagonists in the treatment of cancer. Br J Pharmacol. 2011; 163:220–233. [PubMed: 21232046]
11. Larson SR, Zhang X, Dumpit R, et al. Characterization of osteoblastic and osteolytic proteins in prostate cancer bone metastases. Prostate. 2013; 73:932–940. [PubMed: 23334979]
12. Feeley BT, Gamradt SC, Hsu WK, et al. Influence of BMPs on the formation of osteoblastic lesions in metastatic prostate cancer. J Bone Miner Res. 2005; 20:2189–2199. [PubMed: 16294272]
13. Ishibe M, Rosier RN, Puzas JE. Human prostatic acid phosphatase directly stimulates collagen synthesis and alkaline phosphatase content of isolated bone cells. J Clin Endocrinol Metab. 1991; 73:785–792. [PubMed: 1653783]
14. Kirschenbaum A, Liu XH, Yao S, Leiter A, Levine AC. Prostatic acid phosphatase is expressed in human prostate cancer bone metastases and promotes osteoblast differentiation. Ann N Y Acad Sci. 2011; 1237:64–70. [PubMed: 22082367]
15. Genetos DC, Rao RR, Vidal MA. Betacellulin inhibits osteogenic differentiation and stimulates proliferation through HIF-1alpha. Cell Tissue Res. 2010; 340:81–89. [PubMed: 20165885]
16. Kim HS, Shin HS, Kwak HJ, Cho CH, Lee CO, Koh GY. Betacellulin induces angiogenesis through activation of mitogen-activated protein kinase and phosphatidylinositol 3′-kinase in endothelial cell. FASEB J. 2003; 17:318–320. [PubMed: 12475887]
17. Schneider MR, Mayer-Roenne B, Dahlhoff M, et al. High cortical bone mass phenotype in betacellulin transgenic mice is EGFR dependent. J Bone Miner Res. 2009; 24:455–467. [PubMed: 19049329]
18. Roudier MP, True LD, Higano CS, et al. Phenotypic heterogeneity of end-stage prostate carcinoma metastatic to bone. Hum Pathol. 2003; 34:646–653. [PubMed: 12874759]
19. Zhang X, Morrissey C, Sun S, et al. Androgen receptor variants occur frequently in castration resistant prostate cancer metastases. PLoS ONE. 2011; 6:e27970. [PubMed: 22114732]
20. Kuroda C, Kubota S, Kawata K, et al. Distribution, gene expression, and functional role of EphA4 during ossification. Biochem Biophys Res Commun. 2008; 374:22–27. [PubMed: 18601903]
21. Kawai S, Yamauchi M, Wakisaka S, Ooshima T, Amano A. Zinc-finger transcription factor odd-skipped related 2 is one of the regulators in osteoblast proliferation and bone formation. J Bone Miner Res. 2007; 22:1362–1372. [PubMed: 17547533]
22. Yoshiko Y, Maeda N, Aubin JE. Stanniocalcin 1 stimulates osteoblast differentiation in rat calvaria cell cultures. Endocrinology. 2003; 144:4134–4143. [PubMed: 12933688]
23. Billiard J, Way DS, Seestaller-Wehr LM, Moran RA, Mangine A, Bodine PV. The orphan receptor tyrosine kinase Ror2 modulates canonical Wnt signaling in osteoblastic cells. Mol Endocrinol. 2005; 19:90–101. [PubMed: 15388793]
24. Dhodapkar MV, Abe E, Theus A, et al. Syndecan-1 is a multifunctional regulator of myeloma pathobiology: control of tumor cell survival, growth, and bone cell differentiation. Blood. 1998; 91:2679–2688. [PubMed: 9531576]
25. Lisignoli G, Manferdini C, Codeluppi K, et al. CCL20/CCR6 chemokine/receptor expression in bone tissue from osteoarthritis and rheumatoid arthritis patients: different response of osteoblasts in the two groups. J Cell Physiol. 2009; 221:154–160. [PubMed: 19492413]
26. Bijsterbosch J, Kloppenburg M, Reijnierse M, et al. Association study of candidate genes for the progression of hand osteoarthritis. Osteoarthr Cartil. 2013; 21:565–569. [PubMed: 23357225]
27. Kato K, Nishimasu H, Okudaira S, et al. Crystal structure of Enpp1, an extracellular glycoprotein involved in bone mineralization and insulin signaling. Proc Natl Acad Sci USA. 2012; 109:16876–16881. [PubMed: 23027977]
28. Erlandsen H, Ames JE, Tamkenath A, et al. Pleiotrophin expression during odontogenesis. J Histochem Cytochem. 2012; 60:366–375. [PubMed: 22382872]

29. Seitz S, Rendenbach C, Barvencik F, et al. Retinol deprivation partially rescues the skeletal mineralization defects of Phex-deficient Hyp mice. Bone. 2013; 53:231–238. [PubMed: 23266491]
30. Ariizumi T, Ogose A, Kawashima H, et al. Expression of podoplanin in human bone and bone tumors: new marker of osteogenic and chondrogenic bone tumors. Pathol Int. 2010; 60:193–202. [PubMed: 20403045]
31. Clarkin CE, Gerstenfeld LC. VEGF and bone cell signalling: an essential vessel for communication? Cell Biochem Funct. 2013; 31:1–11. [PubMed: 23129289]
32. Beers SA, Schwender CF, Loughney DA, Malloy E, Demarest K, Jordan J. Phosphatase inhibitors–III. benzylaminophosphonic acids as potent inhibitors of human prostatic acid phosphatase. Bioorg Med Chem. 1996; 4:1693–1701. [PubMed: 8931939]
33. Vovk AI, Mischenko IM, Tanchuk VY, et al. Stereoselectivity of binding of alpha-(N-benzylamino)benzylphosphonic acids to prostatic acid phosphatase. Bioorg Med Chem Lett. 2008; 18:4620–4623. [PubMed: 18672366]
34. Thudi NK, Martin CK, Murahari S, et al. Dickkopf-1 (DKK-1) stimulated prostate cancer growth and metastasis and inhibited bone formation in osteoblastic bone metastases. Prostate. 2011; 71:615–625. [PubMed: 20957670]
35. Wittrant Y, Theoleyre S, Chipoy C, et al. RANKL/RANK/OPG: new therapeutic targets in bone tumours and associated osteolysis. Biochim Biophys Acta. 2004; 1704:49–57. [PubMed: 15363860]
36. Monroe DG, Gee-Lawrence ME, Oursler MJ, Westendorf JJ. Update on Wnt signaling in bone cell biology and bone disease. Gene. 2012; 492:1–18. [PubMed: 22079544]
37. Muniyan S, Chaturvedi NK, Dwyer JG, Lagrange CA, Chaney WG, Lin MF. Human prostatic acid phosphatase: structure, function and regulation. Int J Mol Sci. 2013; 14:10438–10464. [PubMed: 23698773]
38. Metz-Estrella D, Jonason JH, Sheu TJ, Mroczek-Johnston RM, Puzas JE. TRIP-1: a regulator of osteoblast function. J Bone Miner Res. 2012; 27:1576–1584. [PubMed: 22460930]
39. Sheu TJ, Schwarz EM, Martinez DA, et al. A phage display technique identifies a novel regulator of cell differentiation. J Biol Chem. 2003; 278:438–443. [PubMed: 12403789]
40. Chuang TD, Chen SJ, Lin FF, et al. Human prostatic acid phosphatase, an authentic tyrosine phosphatase, dephosphorylates ErbB-2 and regulates prostate cancer cell growth. J Biol Chem. 2010; 285:23598–23606. [PubMed: 20498373]
41. Chaves Neto AH, Queiroz KC, Milani R, et al. Profiling the changes in signaling pathways in ascorbic acid/beta-glycerophosphate-induced osteoblastic differentiation. J Cell Biochem. 2011; 112:71–77. [PubMed: 20626033]
42. Pinkas-Kramarski R, Lenferink AE, Bacus SS, et al. The oncogenic ErbB-2/ErbB-3 heterodimer is a surrogate receptor of the epidermal growth factor and betacellulin. Oncogene. 1998; 16:1249–1258. [PubMed: 9546426]
43. Gross M, Higano C, Pantuck A, et al. A phase II trial of docetaxel and erlotinib as first-line therapy for elderly patients with androgen-independent prostate cancer. BMC Cancer. 2007; 7:142. [PubMed: 17662137]
44. Lin SH, Cheng CJ, Lee YC, et al. A 45-k Da ErbB3 secreted by prostate cancer cells promotes bone formation. Oncogene. 2008; 27:5195–5203. [PubMed: 18490922]
45. Chen D, Li Y, Zhou Z, et al. Synergistic inhibition of wnt pathway by HIF-1alpha and osteoblast-specific transcription factor osterix (Osx) in osteoblasts. PLoS ONE. 2012; 7:e52948. [PubMed: 23300831]

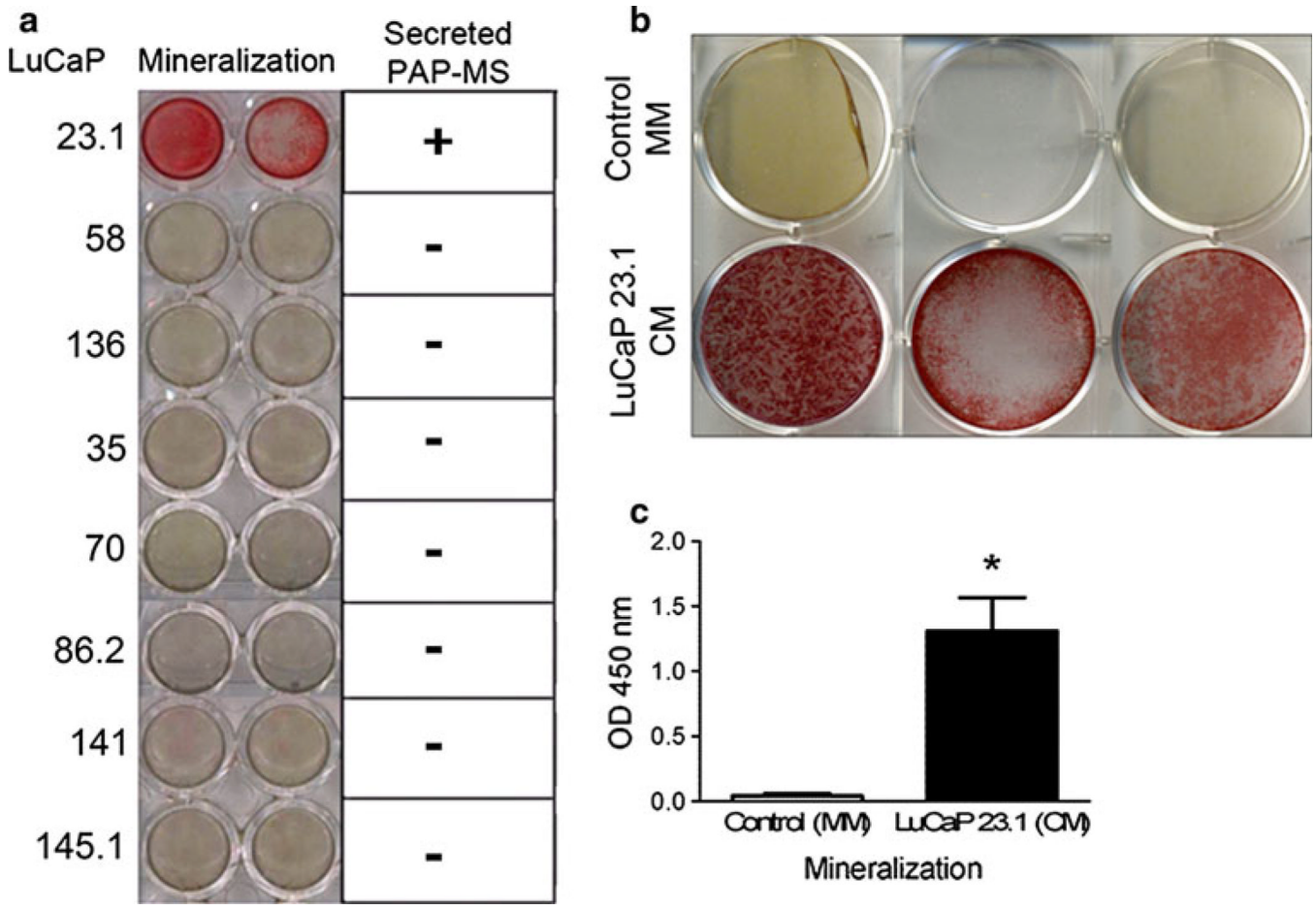

Fig. 1. LuCaP 23.1 induces mineralization in MC3T3-E1 mouse cells, secreting extracellular PAP

a Alizarin Red experiments show that only LuCaP 23.1 promotes mineralization in MC3T3-E1 mouse osteoblast like cells. Mass spectrometry results also indicate that only LuCaP 23.1 secretes sufficient detectable PAP. **b** Alizarin Red staining show that LuCaP 23.1 conditioned media (CM) also promotes mineralization in HCO cells. **c** Graph displaying HCO cells in presence of LuCaP 23.1 significantly promotes mineralization compared to HCO cells in presence of mineralization media (MM) (*p = 0.0079)

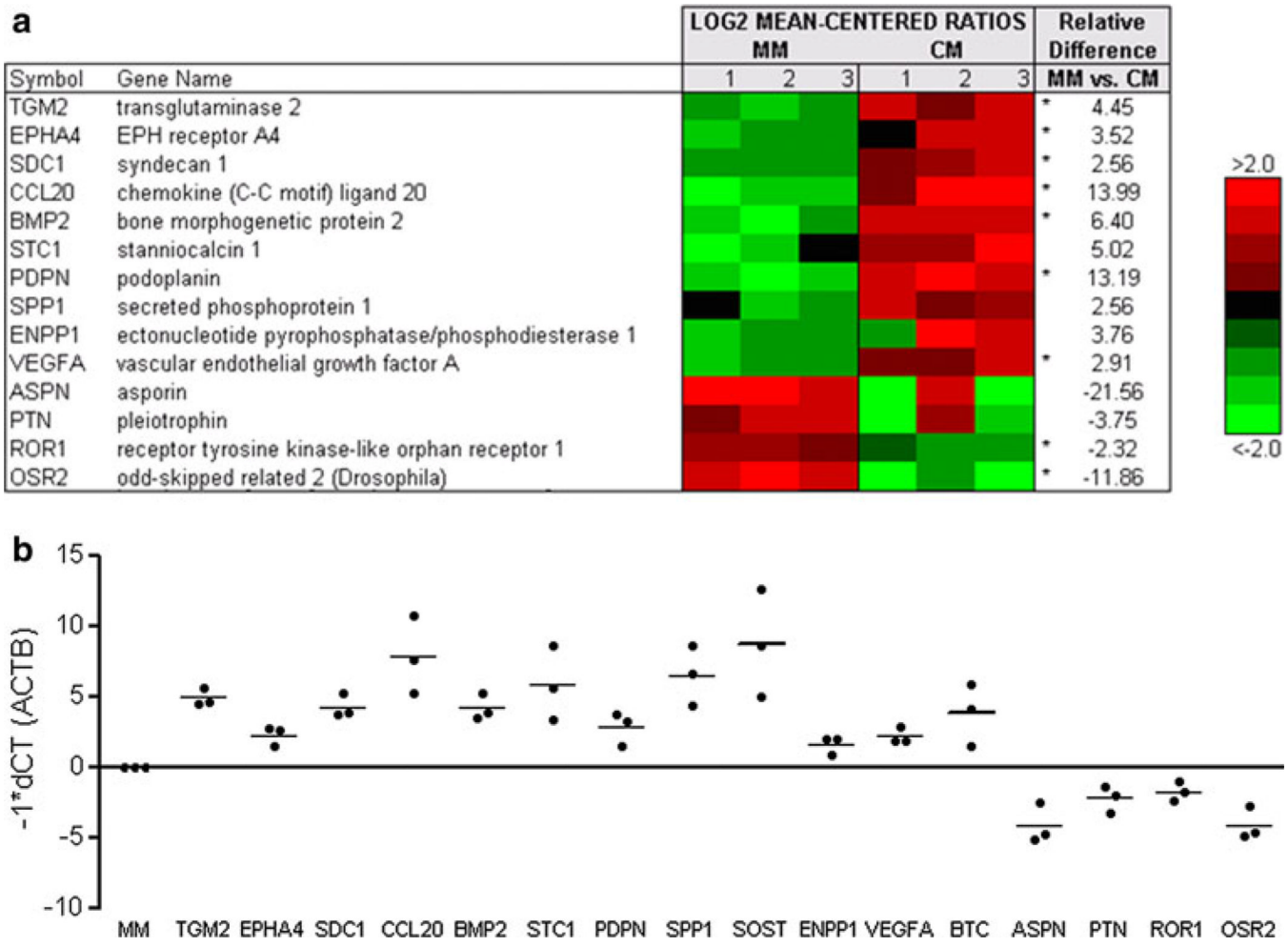

Fig. 2. Expression of mineralization-associated genes in presence of LuCaP 23.1 conditioned media (CM)

a Agilent whole human genome microarrays were used to profile human bone marrow stromal cells (BMSC) from three donors in the presence of mineralization media (MM) or LuCaP 23.1 CM. Mean-centered ratios of 14 genes are colored according to scale. *Probes returning significance in signal strength ($p < 0.05$) using paired t test. **b** qRT-PCR validation for genes of interest. All samples shown were normalized against β-actin and MM and all samples were significantly different from MM alone ($p < 0.05$)

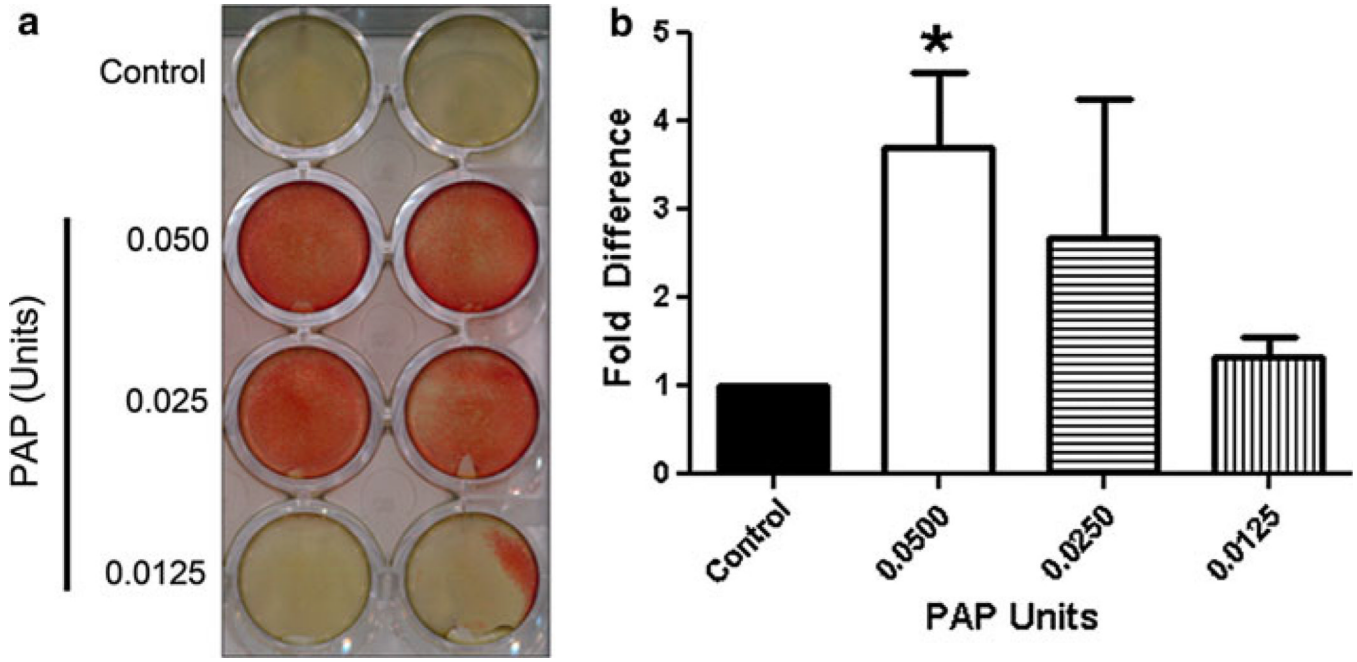

Fig. 3. PAP induces mineralization in mouse osteoblast-like MC3T3-E1 cells

a Alizarin red staining shows that PAP induces mineralization in MC3T3-E1 cells. **b** Graph displaying alizarin red staining of mineralization induced by PAP. Experiments were repeated three times (*p = 0.005)

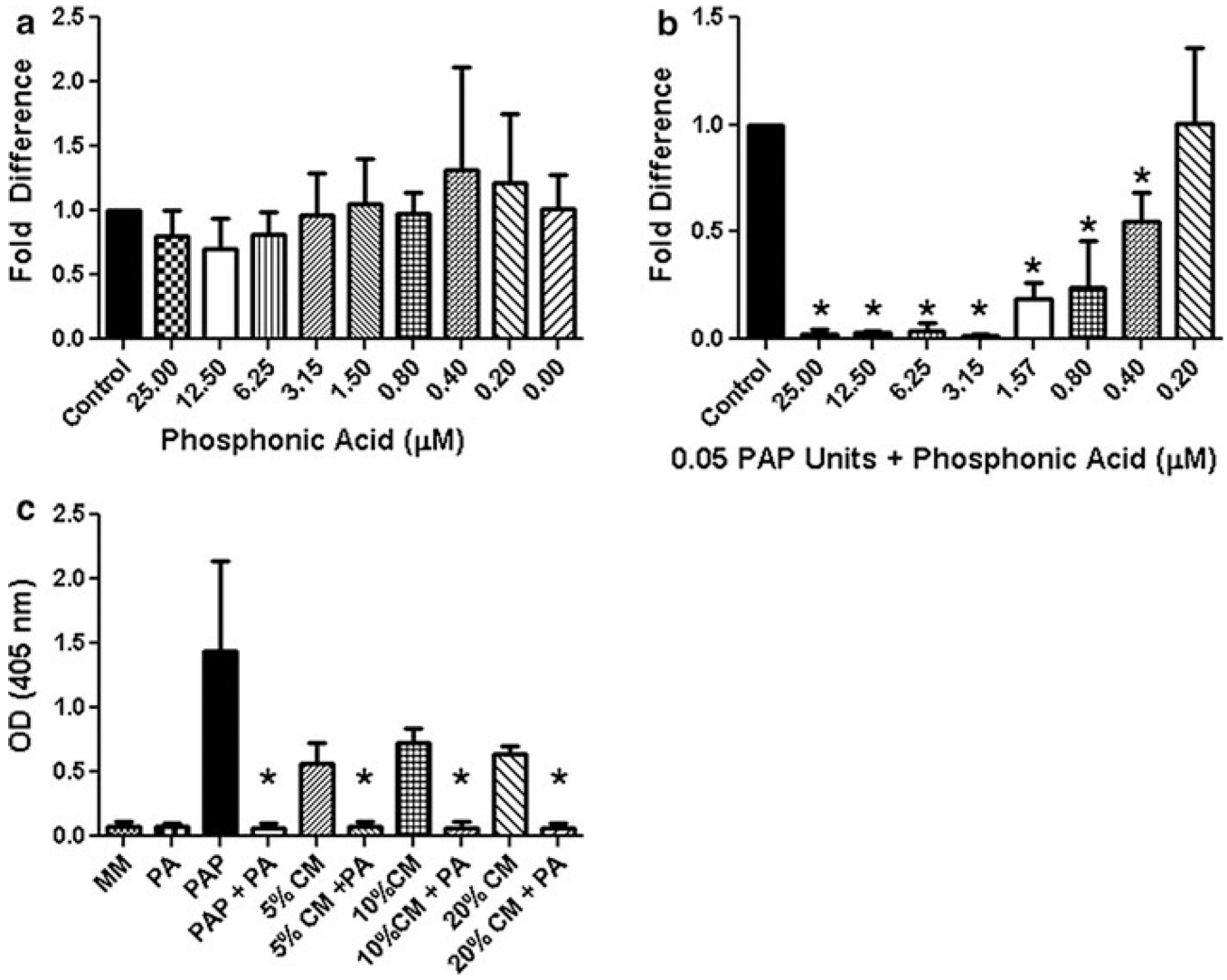

Fig. 4. Phosphonic acid (PA) a PAP inhibitor reduces mineralization

a PA has no significant effects on mineralization when added to MC3T3-E1 cells themselves at concentrations, ranging 25–0.2 μM. **b** MC3T3-E1 cells treated with 0.05 units of PAP were inhibited by PA concentrations ranging from 25 to 0.4 μM PA ($p < 0.05$). **c** Varying concentrations of LuCaP 23.1 conditioned media (CM) (5, 10 and 20 %) uniformly reduced mineralization in presence of 5 μM PA. Experiments were performed three times (*$p < 0.05$)

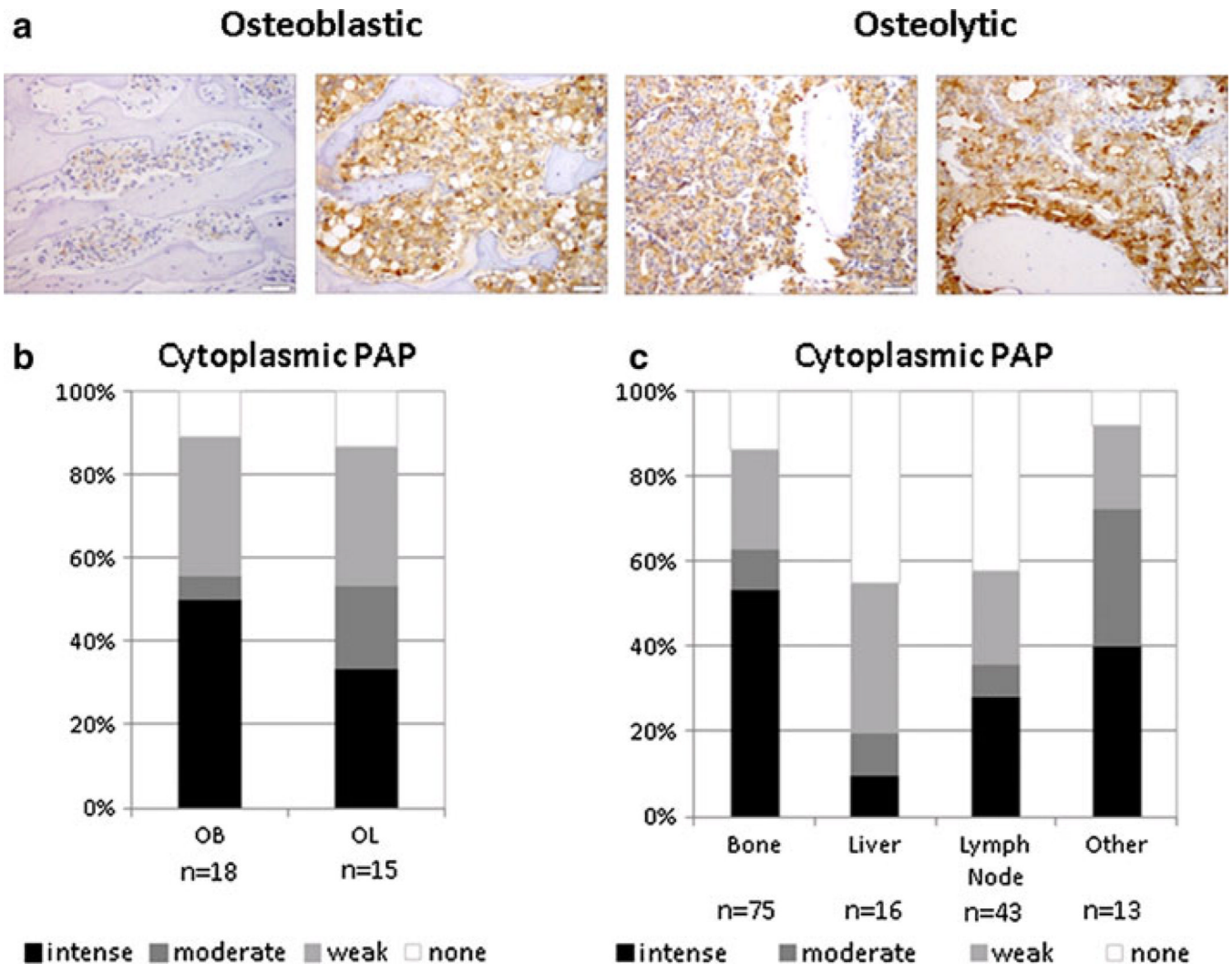

Fig. 5. PAP expression in human PCa metastases

a Representative IHC staining of PAP in osteoblastic and osteolytic PCa bone metastases. Scale bar is equal to 50 μm. **b** Statistical analysis reveals no significant difference in the expression of PAP between the osteoblastic and osteolytic bone metastases ($p = 0.749$). Staining intensity ranges from none (*white*) to intense (*black*). **c** Statistical analysis of PAP expression in tumor metastases from bone, liver, lymph nodes, and other tissues (appendix, lung and kidney). Expression of PAP was higher in bone metastases compared to other metastatic sites, such as liver ($p < 0.001$) and lymph nodes ($p < 0.001$) with no difference observed between bone and other sites (appendix, kidney and lung) ($p = 0.969$)

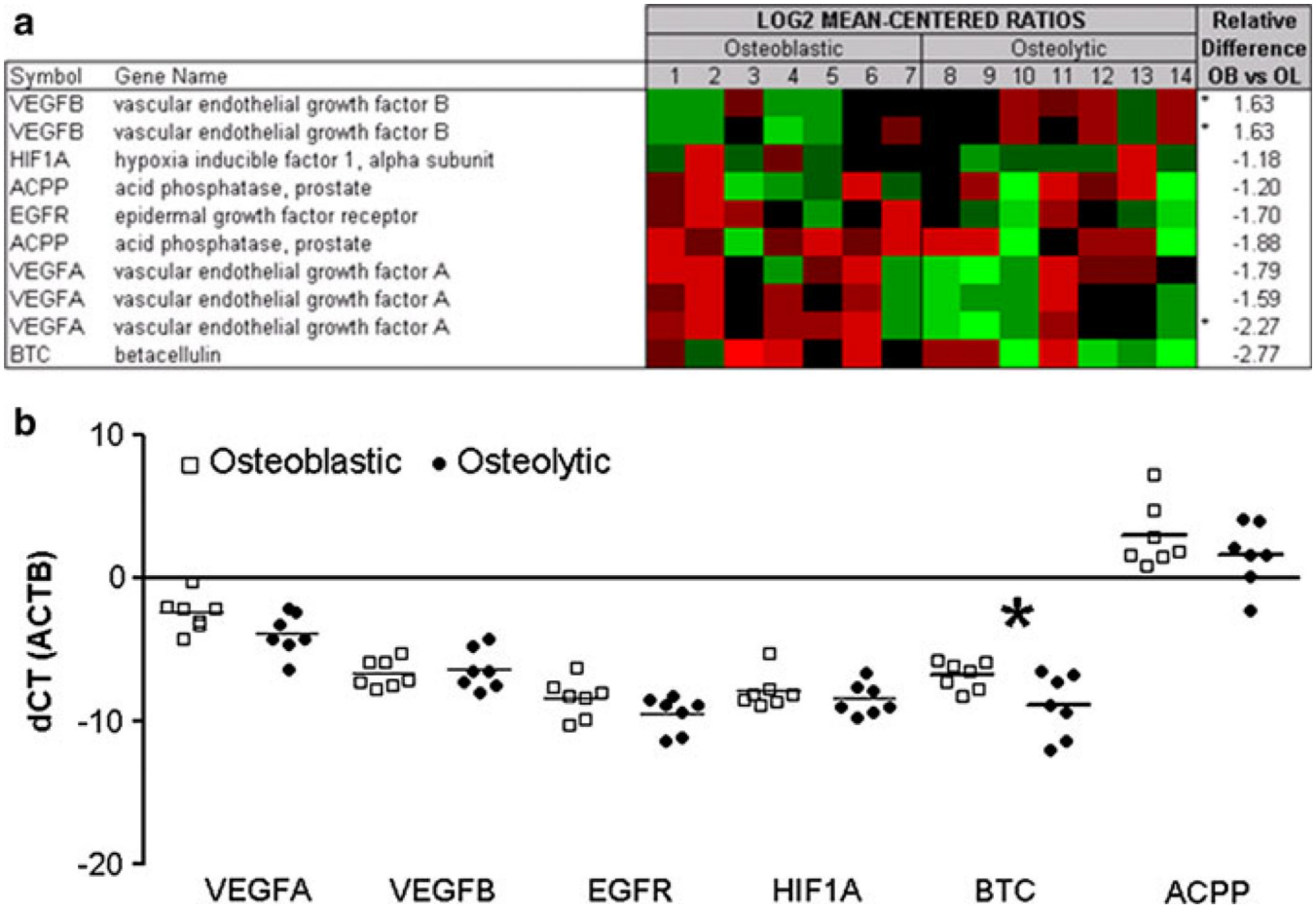

Fig. 6. Transcript expression of BTC and BTC-associated proteins

a Agilent whole human genome microarrays were used to profile seven highly osteoblastic and seven highly osteolytic bone metastases. Mean-centered ratios of known and novel bone remodeling genes are colored according to scale. *Probes returning significance in signal strength ($p < 0.05$) using paired t-test. **b** Validation of microarrays by qRT-PCR in osteoblastic (*white squares*) and osteolytic (*black circles*) PCa metastases. All samples are normalized against β-actin. *Indicates significant difference with a p-value of $p < 0.05$

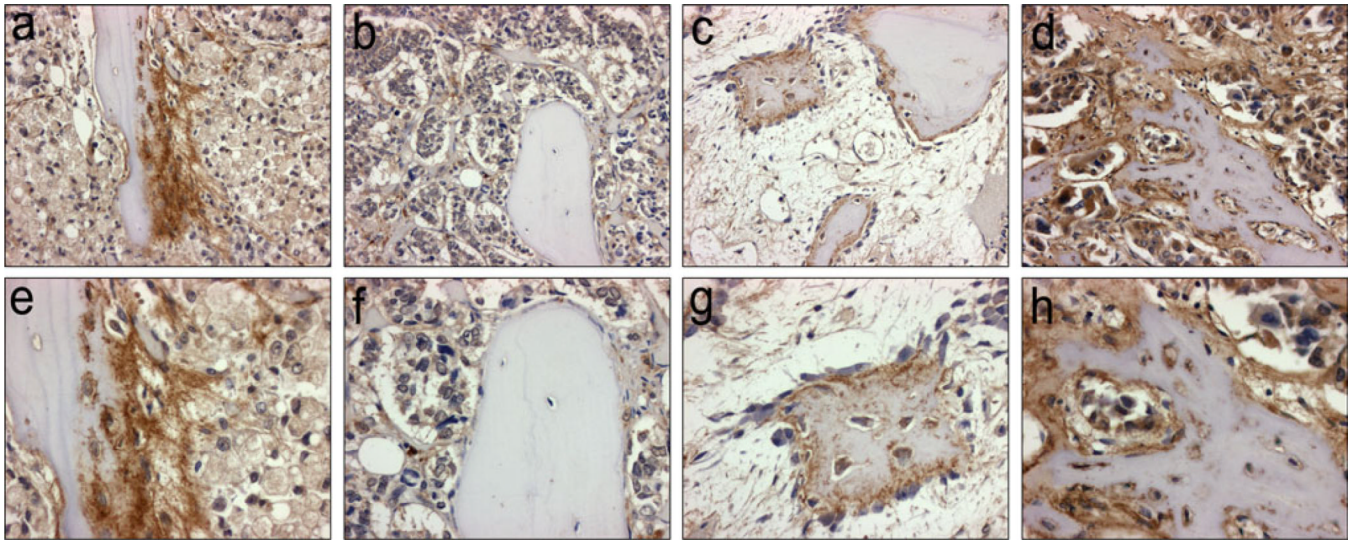

Fig. 7. Betacellulin (BTC) expression is associated with new bone growth in clinical samples of PCa bone metastases

a, **e** New bone formation on older lamellar bone. Osteoblasts, osteocytes, and tumor stroma are strongly positive for BTC (*brown stain*), tumor cells stain weakly. **b**, **f** Old lamellar bone in the center of a PCa bone metastasis (limited BTC expression is observed in all cell types). **c**, **g** New bone formation in the reactive bone marrow stroma of an osteoblastic PCa bone metastasis. Osteoblasts and osteocytes are positive for BTC. **d**, **h** Strong BTC expression is present in tumor cells, osteoblasts, osteocytes, and new bone. Magnification: Panel **a**–**d** X200; Panel **e**–**h** X400